Multibody Syst Dyn (2008) 19: 255–280
DOI 10.1007/s11044-007-9057-3

Clearance and friction-induced dynamics of chain CVT drives

Nilabh Srivastava · Imtiaz Haque

Received: 20 November 2006 / Accepted: 18 April 2007 /
Published online: 17 July 2007

Abstract A continuously variable transmission (CVT) is an emerging automotive transmission technology that offers a continuum of gear ratios between desired limits. A chain CVT is a friction-limited drive as its performance and torque capacity rely significantly on the friction characteristic of the contact patch between the chain and the pulley. Moreover, such a CVT is susceptible to clearance formation due to assembly defects or extensive continual operation of the system, which further degrades its performance and leads to early wear and failure of the system. The present research focuses on developing models to understand the influence of clearance and different friction characteristics on the dynamic performance of a chain CVT drive. A detailed planar multibody model of a chain CVT is developed in order to accurately capture the dynamics characterized by the discrete structure of the chain, which causes polygonal excitations in the system. A suitable model for clearance between the chain links is embedded into this multibody model of the chain CVT. Friction between the chain link and the pulley sheaves is modeled using different mathematical models which account for different loading scenarios. The mathematical models, the computational scheme, and the results corresponding to different loading scenarios are discussed. The results discuss the influence of friction characteristics and clearance parameters on the dynamic performance, the axial force requirements, and the torque transmitting capacity of a chain CVT drive.

Keywords Continuously variable transmission · CVT · Chain · Friction · Stribeck effect · Pulley · Multibody · Nonlinear dynamics · Clearance

Abbreviations

a	Starting coefficient of friction between chain and pulley ($\sim$0.003)
$1/b, \kappa$	Rate of growth of friction coefficient, μ
(x_c, y_c)	Coordinates of the center of mass of a link
θ	Rotational degree of freedom of a link
(ac_x, ac_y)	Linear acceleration of the center of mass of a link

N. Srivastava (✉) · I. Haque
Clemson University, 106 EIB, Flour Daniel Bldg., Clemson, SC 29634, USA
e-mail: snilabh@clemson.edu

m	Mass of a chain link
I_c	Moment of inertia of a chain link about its center of mass
λ_N, N	Normal force between a chain link and a pulley
λ_T	Force during the sticking phase of a contact
J_p	Pulley rotational inertia
φ	Pulley rotational coordinate
β_0	Half-sheave angle of non-deformed pulley
β	Half-sheave angle of deformed pulley
θ_c	Angular location of center of wedge-expansion
Δ	Amplitude of the sheave angle sinusoid
τ	Torque on the driver pulley
r, r'	Link pitch radius on driver and driven pulleys
z	Local distance between the pulley surfaces
u	Axial width variation due to pulley flexibility
v_{rel}	Relative velocity between the contacting surfaces
ζ	Angular location of a link over the pulley wrap
k, p	Stiffness and damping parameters of the interconnecting force element
ε	Clearance between the chain-links
μ	Coefficient of friction between link and pulley
μ_0	Coefficient of kinetic friction between link and pulley
σ	Parameter related to the ratio of the coefficients of static and kinetic friction
χ	Stribeck-effect/lubrication parameter
γ	Sliding angle
$\mathbf{M}$	Mass matrix (assembled)
$\mathbf{h}$	Forcing vector containing contributions from active forces/torques and other gyroscopic terms

1 Introduction

Over the past two decades, continuously variable transmissions (CVTs) have aroused a great deal of interest in the automotive sector due to the potential of lower emissions and better performance. A CVT is an emerging automotive transmission technology that offers an infinite number of gear ratios between two limits, which consequently allows better matching of the engine operating conditions to the variable driving scenarios. A CVT offers potential advantages over the conventional automatic and manual transmissions, chiefly: higher engine efficiency, better fuel economy, low cost, and infinite gear ratios with fewer parts. Today several auto manufacturers, such as Honda, Toyota, Ford, Nissan, etc., are already keen on exploiting the various advantages of a CVT in a real production vehicle. In spite of the several advantages proposed by a CVT system, the complete potential of a CVT, in terms of the mass production and market penetration of CVT-equipped vehicles, has not been realized so far. In order to achieve lower emissions and better performance, it is necessary to understand the dynamic interactions occurring in a CVT system in detail, so that efficient controllers could be designed to overcome the existing losses and enhance vehicle fuel economy. Moreover, it is of interest to know how the performance and torque capacity of a CVT system gets affected as its components begin to wear out due to continual operation, wear, or fatigue.

A chain CVT consists of two variable-diameter pulleys kept at a fixed distance apart and connected to each other by a chain. One of the sheaves on each pulley is movable. The chain

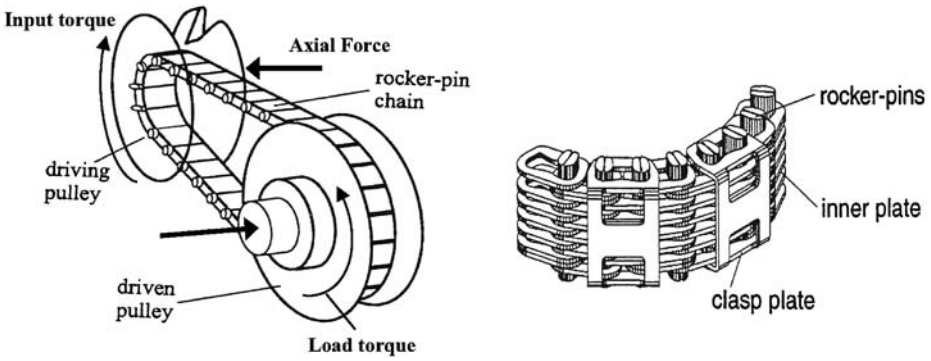

Fig. 1 Chain CVT and chain link configuration [1]

can undergo both radial and tangential motions, depending on the loading conditions and the axial forces applied to the pulley sheaves. The pulley on the engine side is called the driver pulley and the one on the final drive side is called the driven pulley. Figure 1 depicts the chain structure and the basic configuration of a chain CVT drive. A rocker-pin chain consists of plates and rocker pins, as depicted in the figure. All plates and pins transmit tractive power. The plates also prevent rocking of the pins by orienting them perpendicular to the direction of motion of the chain. Owing to the discrete structure of a chain, the contact forces between the pins and the pulleys are discretely distributed. Consequently, impact-related vibrations occur as chain links enter and leave the pulley. These excitation mechanisms, which are related to the polygonal action of chain links, significantly influence the performance of a chain CVT drive.

As mechanical systems wear, clearances between mating surfaces develop that can fundamentally change the behavior of the system and also induce unnecessary noise and vibrations [2–4]. A CVT is no exception, and over continual operation it is susceptible to form clearances between its components. Moreover, it is quite possible for a CVT to have clearances among its various components during the assembly process. These clearances influence the dynamic behavior, torque capacity, and life of a CVT. Clearance inherently is a nonsmooth nonlinearity (may be piecewise linear), which makes the CVT system nonsmooth too.

A chain CVT falls under the category of friction-limited drives as its performance and torque capacity rely significantly on the friction characteristic of the contact patch between the chain and the pulley. The torque capacity of a friction-driven CVT (i.e., belt or chain CVT) is limited by the strength of the belt or chain and the ability to withstand friction wear between the source and transmission medium. Much research is being conducted on different aspects of a CVT, e.g., performance, slip behavior, efficiency, configuration design, loss mechanisms, vibrations, etc. Although a lot of work has been done on capturing the influence of clearance on the dynamics of metal V-belt CVTs [5–12], literature pertaining to clearance and friction-related dynamics of chain CVT drives is scarce [13, 14]. Fawcett [15] did an extensive review on the existing literature related to belt and chain drives. The papers from different sources were grouped into three sections: dynamics of axially moving materials, chain-drive dynamics, and belt-drive dynamics. Most of the literature discussed by the author was related to the dynamics of roller chain drives, rubber V- and flat belts, and toothed belts. Srnik and Pfeiffer [1, 16] studied the dynamic behavior of a CVT chain drive for high torque applications. They developed a planar model of chain CVT with three-dimensional contact between chain link and pulley. The work dealt with multi-body formalisms and finite

element modeling. The chain links were modeled as kinematically decoupled rigid bodies, which were interconnected by force elements, as proposed by Fritz and Pfeiffer [17]. Sauer [16] developed a finite-element method (FEM) based, static model for a CVT chain drive with elastic pulley-sets and a chain described link by link. The model gives a good theoretical description of the torque transfer behavior of CVT chain drives. Sedlmayr and Pfeiffer [18, 19] extended the previous work done by Srnik and Pfeiffer [1] to include the effects of spatial orientation on the dynamics of CVT chain drives. The authors modeled the links and the pulleys as elastic bodies and also included pulley misalignment effects. Sattler [20] analyzed the mechanics of a metal chain and V-belt considering both longitudinal and transverse stiffness of the chain and belt, and misalignment and deformation of the pulley. The pulley deformation is modeled using a standard finite-element analysis. The pulley is assumed to deform in two ways, pure axial deformation and a skew deformation. The model was also used to study efficiency aspects of belt and chain CVTs. A comparative study on the dynamics and performance of metal V-belt CVT and chain CVT was done by Lebrecht et al. [21]. Tenberge [22] developed a fast computational algorithm to compute dynamic indicators of chain CVT from a mathematical model which includes deformations, loadings, and other inertial effects at constant and variable speed ratios. Lebrecht et al. [23] analyzed self-induced vibrations in a pushing V-belt CVT by using highly simplified friction models. It was shown that the certain friction characteristics, especially those having negative gradient with respect to relative velocity, could induce self-excited vibration in the belt. The friction characteristic and the elasticity of the pulley sheaves also determined the working area where vibrations occurred.

Although the friction characteristic of the contacting surface inevitably plays a crucial role on CVT's performance, literature pertaining to the influence of friction characteristic on CVT dynamics is scarce [6, 12, 14, 23, 24]. With a few exceptions, almost all the models mentioned in the literature use Coulomb friction theory to model friction between the contacting surfaces of a CVT. However, depending on different operating (or loading) conditions and design configurations, the friction characteristic of the contacting surface may vary. For instance, in case of a fully lubricated CVT, the friction characteristic of the contacting surface may bear a resemblance to the Stribeck curve [25] rather than to a continuous Coulomb characteristic. Moreover, very high forces in the contact zone may further lead to the conditions of elasto-plastic-hydrodynamic lubrication, which may yield a different friction characteristic. It has also been briefly reported [23] in the literature that certain friction characteristics induce self-excited vibrations in the CVT system. However, it is not clear whether such a phenomenon is an artifact of the friction model or the real behavior of the system. It is thus necessary to study the influence of different friction characteristics on the performance of a transient-dynamic model of a chain CVT. It is also important to note that although an exact knowledge of the friction characteristic in a CVT system can only be obtained by conducting experiments on a real production CVT, these mathematical models give profound insight into the probable behavior that a CVT system exhibits under different operating conditions, which may be further exploited to design more efficient controllers.

The research reported in this paper focuses on the development of a detailed dynamic model of a chain CVT using multibody formalisms. Since excitation mechanisms exist due to the impact and polygonal action of chain links in a chain CVT, it is necessary to model the chain CVT as a multibody system in order to accurately capture the dynamics arising from its discrete nature. The chain CVT model is developed using Pfeiffer and Glocker's theory [26] on multibody dynamics with unilateral contacts. Since it is experimentally cumbersome to measure the exact friction characteristics of the contacting surfaces in a CVT system, different literature-based mathematical models of friction will be incorporated into

the transient-dynamic CVT model in order to gain an insight into the influence of friction on the dynamic performance of a CVT. Moreover, since clearance-related dynamics have not been explored previously in a chain CVT system, a clearance model is embedded into this model in order to study the influence of clearance parameters on the performance of a chain CVT drive. The goal is to understand the transient dynamic behavior of a chain CVT drive as the chain links traverse the contacting arcs over the driver and driven pulleys and to also evaluate the system performance under the influence of clearance and different contact-zone friction characteristics. The modeling analysis and the results corresponding to the chain CVT model are discussed in detail in the subsequent sections.

2 Modeling of a chain CVT

As depicted in Fig. 1, a chain CVT consists of two variable-diameter pulleys connected to each other by a chain. The system is subjected to an input torque on the driver pulley and a resisting load torque on the driven pulley. The model captures various dynamic interactions between a chain link and the pulley as the link moves from the entrance to the exit of the pulley. The model development and analysis includes the following assumptions:

- The pulleys do not have any misalignment between them
- The chain links are rigid
- The interactions between the rocker pins of neighboring links and between a rocker pin and a plate can all be accounted for by modeling the chain link as a planar rigid body
- Negligible out-of-plane interaction of chain links
- Bending and torsional stiffness of the chain links are neglected

The modeling of various components of a chain-drive CVT is discussed subsequently.

2.1 Model of chain links

The chain in the CVT is modeled link by link to account for its discrete structure. Each chain link represents a rigid body with three degrees of freedom in a plane (i.e. $(x_c,\ y_c,\ \theta)$): two translations of the center of mass of the link and one rotation about an axis passing through the link's center of mass. The chain links are connected to each other by force elements which take into account the elasticity and damping of the links and joints. In case of contact between a link and a pulley, additional normal and tangential forces act on the bolt of the link and therefore on the link. These contact forces correspond with the associated contact forces acting on the pulley. The force element between the links is governed by a nonlinear force-deformation law (like a hardening spring) in order to take the dynamic effects due to clearance between the links into account. Figures 2 and 3 illustrate the free-body diagram of a chain link.

It is to be noted that in Fig. 2, the dotted arrows represent the forces (f_x and f_y), which only arise when a chain link comes in contact with the pulley sheave. Using Newton–Euler equations, the equation of motion of a link not in contact with pulley can be written in matrix form in terms of generalized coordinates $\mathbf{q}$ as:

$$\mathbf{J}^{\mathbf{T}}\begin{bmatrix} m\mathbf{E} & \mathbf{0} \\ \mathbf{0} & \mathbf{I}_{\mathrm{C}} \end{bmatrix}\mathbf{J}\ddot{\mathbf{q}} + \mathbf{J}^{\mathbf{T}}\begin{bmatrix} \mathbf{0} \\ \tilde{\boldsymbol{\Omega}}\mathbf{I}_{\mathrm{C}}\boldsymbol{\Omega} \end{bmatrix} = \mathbf{J}_{\mathrm{A,B}}^{\mathrm{T}}\begin{bmatrix} \mathbf{F} \\ \tilde{\mathbf{r}}_{\mathrm{A,B}}\mathbf{F} \end{bmatrix}. \tag{1}$$

The generalized coordinates $\mathbf{q}$ for a link are $(x_c,\ y_c,\ \theta)$. The position vector of a point on the link from its center of mass C is denoted by $\mathbf{r}$. The link mass and moment of inertia

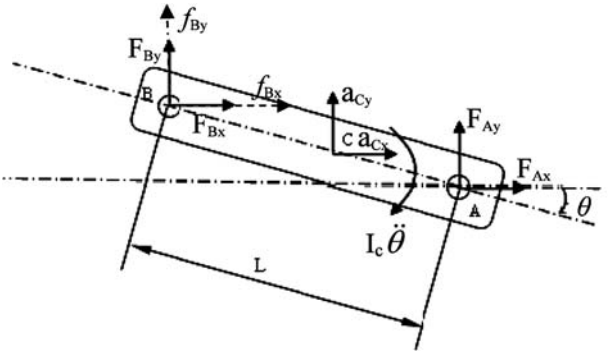

Fig. 2 Free body diagram of a chain link

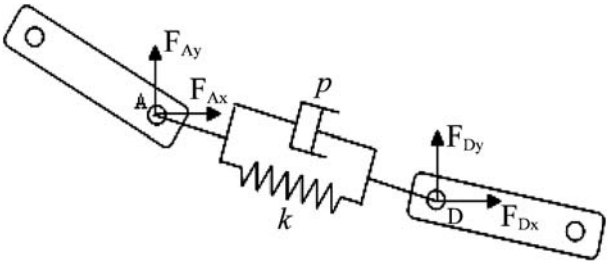

Fig. 3 Free body diagram of chain link interaction

tensor about its center of mass is denoted by m and $\mathbf{I_c}$ respectively. $\mathbf{E}$ denotes the identity matrix. The Jacobian matrix $\mathbf{J}$ between the system coordinates and the configuration (or generalized) coordinates of a link at its center of mass can be obtained as

$$\mathbf{v_C} = \begin{bmatrix} \dot{x}_C \\ \dot{y}_C \\ 0 \end{bmatrix}, \qquad \mathbf{\Omega} = \begin{bmatrix} 0 \\ 0 \\ \dot{\theta} \end{bmatrix}, \qquad \dot{\mathbf{q}} = \begin{bmatrix} \dot{x}_C \\ \dot{y}_C \\ \dot{\theta} \end{bmatrix},$$
$$\mathbf{J} = \begin{bmatrix} \mathbf{J}_\mathrm{C} \\ \mathbf{J}_\mathrm{R} \end{bmatrix} = \begin{bmatrix} \frac{\partial \mathbf{v_C}}{\partial \dot{\mathbf{q}}} \\ \frac{\partial \mathbf{\Omega}}{\partial \dot{\mathbf{q}}} \end{bmatrix} = \begin{bmatrix} 1 & 0 & 0 \\ 0 & 1 & 0 \\ 0 & 0 & 0 \\ 0 & 0 & 0 \\ 0 & 0 & 0 \\ 0 & 0 & 1 \end{bmatrix}. \tag{2}$$

Similarly, Jacobian matrices in a link at the points of application of the active force $\mathbf{F}$ (A, B in the figure) can be obtained through the velocities of the corresponding points of the link, i.e., $\mathbf{J}_A$ can be obtained through an expression for velocity at point A, $\mathbf{v}_A$. The active forces $\mathbf{F}$ and the torques acting on a link due to these forces are obtained by computing the forces in springs and dampers of the force-elements connecting to that particular link. Now, summing (1) for all those links not in contact with the pulley will yield the following equation of motion for the multi-degree-of-freedom system:

$$\mathbf{M}(\mathbf{q}, t) \cdot \ddot{\mathbf{q}} - \mathbf{h}(\mathbf{q}, \dot{\mathbf{q}}, t) = \mathbf{0}. \tag{3}$$

However, (3) does not take into account the contact force conditions between a link and the pulley. So, as the links come in contact with the pulley, they generate contact forces,

which modify the equations of motion of the system. Hence, following analysis and notation similar to [26], the equation of motion for all the links under unilateral contact conditions with the pulleys can be written as

$$\mathbf{M}\ddot{\mathbf{q}} - \mathbf{h} - (\mathbf{W}_{\mathrm{N}} + \mathbf{W}_{\mathrm{S}}\hat{\boldsymbol{\mu}}_{\mathrm{S}}|\mathbf{W}_{\mathrm{T}})\begin{bmatrix}\boldsymbol{\lambda}_{\mathrm{N}}\\ \boldsymbol{\lambda}_{\mathrm{T}}\end{bmatrix} = 0 \tag{4}$$

where

$$\hat{\boldsymbol{\mu}}_{\mathrm{S}} = \left\{-\mu_i(\dot{g}_{Ti})\,\mathrm{sign}(\dot{g}_{Ti})\right\}.$$

Here, $\boldsymbol{\lambda}_{\mathrm{N}}$, $\boldsymbol{\lambda}_{\mathrm{T}}$ are the normal and the sticking constraint forces of the links that are in contact with the pulley and $\dot{g}_{Ti}$ is the tangential relative velocity between a link, i, and the pulley. $\mathbf{W}_{\mathrm{N}}$ represents a matrix with coefficients of relative acceleration (in the normal direction) between the links and pulley in the configuration space. $\mathbf{W}_{\mathrm{S}}$ represents a matrix with coefficients of relative acceleration (in the tangential direction) between the links and pulley in the configuration space when the links are slipping on the pulley sheave, whereas $\mathbf{W}_{\mathrm{T}}$ represents a matrix with coefficients of relative acceleration (in the tangential direction) between links and pulley in the configuration space when the links are sticking to the pulley sheave. It is to be noted that the relative velocity and accelerations are computed at the contact points where the links contact the pulley.

2.2 Model of pulleys

Each pulley is modeled as a rigid body with one degree of freedom, i.e., the rotational degree of freedom (φ). A pulley is loaded with the frictional and normal forces acting between the rocker pins of the links and the pulley and also with an external moment. An input torque is applied to the driver pulley and a load torque on the driven pulley. Similar to (4), the equation of motion of a pulley under unilateral contact conditions with the link is given by

$$J_P\ddot{\varphi} = h_P - (\mathbf{W}_{\mathrm{Np}} + \mathbf{W}_{\mathrm{Sp}}\hat{\boldsymbol{\mu}}_{\mathrm{S}}|\mathbf{W}_{\mathrm{Tp}})\begin{bmatrix}\boldsymbol{\lambda}_{\mathrm{Np}}\\ \boldsymbol{\lambda}_{\mathrm{Tp}}\end{bmatrix}. \tag{5}$$

The term, h_P, accounts for the moment contributions from the input and load torques on the pulleys. The terms, $\mathbf{W}_{\mathrm{Np}}$, $\mathbf{W}_{\mathrm{Sp}}$, $\mathbf{W}_{\mathrm{Tp}}$ are analogous to the terms $\mathbf{W}_{\mathrm{N}}$, $\mathbf{W}_{\mathrm{S}}$, $\mathbf{W}_{\mathrm{N}}$ in (4).

Occasionally it has been observed [1, 12–14, 27–29] that the variation of local groove width caused by the elastic deformation of the pulleys significantly influences the thrust ratio and slip behavior of a belt/chain CVT. However, since the primary goal of this research was to study the influence of friction characteristic on CVT dynamics, a detailed finite-element modeling of pulley sheaves was avoided. Hence, instead simple trigonometric functions (as outlined in [12–14, 28, 29]) are used to describe the varying pulley groove angle and the local elastic axial deformations of the pulley sheaves. Figure 4 depicts the model for pulley deformation. The following equations describe pulley deformation effects in Fig. 4:

$$\beta = \beta_0 + \frac{\Delta}{2}\sin\left(\zeta - \theta_c + \frac{\pi}{2}\right). \tag{6}$$

The angular location of a chain link over driver and driven pulley wrap is denoted by ζ in (6). Using this approximation for the sheave angle deformation, the pitch radius of the chain link in the deformed pulley sheave can be easily computed. The amplitude of the variation in the pulley groove angle, Δ, is always much smaller than unity; however, it is not constant

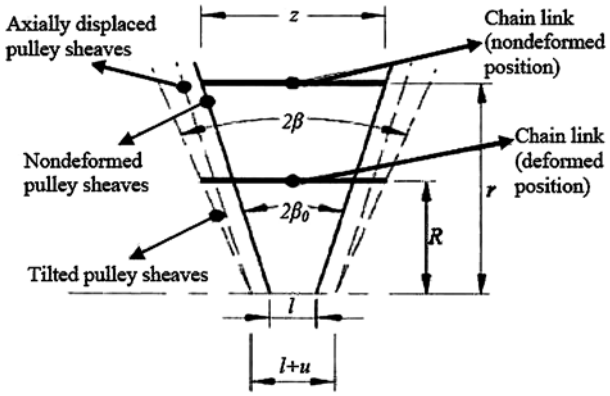

Fig. 4 Pulley deformation model

during speed ratio changing phases due to variation in the pulley axial (clamping) forces. Sferra et al. [29] proposed the following approximate correlations for the variation Δ and the center of the pulley wedge expansion θ_c in terms of the transmitted torque τ and the chain pitch radius on driver and driven pulleys r and r', respectively.

$$\begin{aligned} \Delta &= \frac{0.00045\tau}{(\frac{r}{r'})^{0.55}}, \\ \theta_c &= \frac{\pi}{3}\frac{r}{r'} + \frac{23\pi}{180}. \end{aligned} \tag{7}$$

2.3 Model of link-pulley contact

A chain link contacts a pulley at the ends of a rocker pin. As the plates move, the rocker pins of adjacent links also interact with each other. Assuming negligible dynamic interaction between a pair of rocker pins, these rocker pins are modeled as a single bolt. So, every link is associated with one bolt through which it contacts the pulley sheaves. The bolt is represented as a linear massless spring. The contact planes of the bolts are the end faces of the springs. The surfaces of the bolt are loaded with the normal and frictional contact forces. Figure 5 illustrates the free body diagram for the interactions between the bolt and a pulley. In this figure, $\mathbf{F}_r$ and $\mathbf{F}_t$ represent the components of the resultant friction force vector $\mathbf{F}_f$ between a chain link and the pulley, which act in the plane of the pulley sheave, and $\mathbf{N}$ is the normal force between the link and the pulley.

It is necessary to quantify the bolt spring force F_b in order to derive the contact forces. The bolt force depends on the bolt length l_b and stiffness K_b as well as on the local distance of the pulley's surfaces z. Since the pulley sheaves also bend, additional axial width variation (refer to Fig. 4) affects the bolt force. So, the bolt force F_b can be written as:

$$F_b = \begin{cases} K_b(l_b - z - u) & \forall (z+u) \le l_b, \\ 0, & \forall (z+u) > l_b. \end{cases} \tag{8}$$

It is to be noted that the chain link slips in the plane of the pulley sheave. The slip angle γ defines the plane in which the friction force acts. It is the angle which the resultant friction force vector $\mathbf{F}_f$ makes with the tangential direction vector to the pulley. So, in order to get the friction force vector, it is crucial to keep a track of the relative velocity vector between

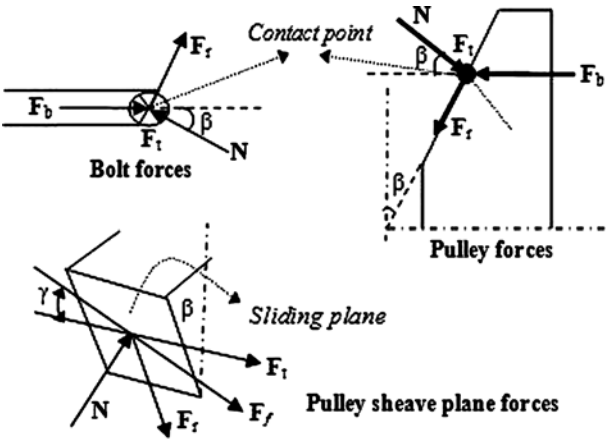

Fig. 5 Link-pulley contact description

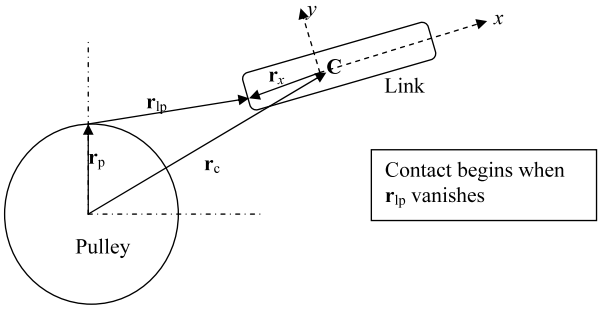

Fig. 6 Contact kinematics between link and pulley

the chain link and the pulley. The relative acceleration and the relative velocity between the link and the pulley can be obtained using the contact kinematics depicted in Fig. 6.

2.4 Model for clearance between links

As mentioned previously, the chain links are modeled as rigid bodies connected to each other by means of force elements, i.e., springs and dampers. Due to repetitive operation, a chain-drive CVT is susceptible to form clearances between links over a period of time. Moreover, assembly operations can also give rise to clearances between the various components of a chain CVT. Link clearance, as depicted in Fig. 7, drastically influences the dynamic behavior of the chain CVT as it affects the transmitted torque and also causes early wear owing to high noise and vibrations in the system. Figure 8 also depicts the force-deformation law in the spring which accounts for the clearance (ε) between the chain link elements. It is obvious from the figure that the clearance among the links influences the total transmitted force in the chain-drive CVT. It is to be noted that in contrast to the ideal case (i.e. zero clearance), the stiffness and damping changes when there is clearance between the links. Moreover, as this clearance gap closes, the stiffness and damping in the interacting force element rises. So, as the clearance gap closes, the spring force increases. Moreover, losses can be associated with link-clearance as the torque transmitted for such CVTs is less than that for a chain CVT with no link-clearance. Clearance can also induce undesirable or perilous nonlinear phenomena in a system, the most common being self-excited vibrations.

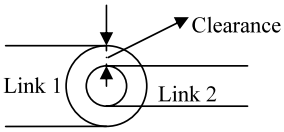

Fig. 7 Chain link clearance

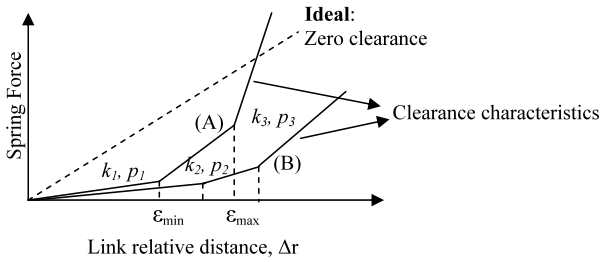

Fig. 8 Clearance model for chain links

2.5 Modeling of friction between a link and the pulley

Almost all the models, except the few mentioned in the literature, use classical the Coulomb–Amonton friction law to model friction between the contacting surfaces of a CVT. The friction phenomenon described by this law is inherently discontinuous in nature. It is common engineering practice to introduce a smoothening function to represent the set-valued friction law. However, certain friction-related phenomena like chaos, limit-cycles, hysteresis, etc., are neither easy to detect nor easy to explain on the basis of classical Coulomb–Amonton friction theory. Since it is difficult to monitor friction experimentally during the running conditions of a complex nonlinear system (e.g., a CVT), mathematical models of friction give insight into the different dynamic maneuvers that a system can undergo.

It is evident that (4) and (5) possess time-varying structure due to the possible transitions between stick and slip phases of the contact. However, without significant loss of accuracy [1], it is possible to evade this time-variance in the system by assuming the friction between the bolt of the chain link and the pulley to be approximated by a smooth nonlinear function. Two different mathematical models are embedded into the multibody model of chain CVT in order to capture friction between the link and the pulley under different operating or loading conditions. Figure 9 depicts the friction characteristics described by these mathematical models.

The coefficient of friction between the link and the pulley is governed by the following relationship:

$$\begin{aligned} &\text{Case 1:} \quad \mu = a + (\mu_o - a)\left(1 - e^{-|v_{rel}|/b}\right), \\ &\text{Case 2:} \quad \mu = \mu_0\left(1 - e^{-\kappa|v_{rel}|}\right)\left(1 + (\sigma - 1)e^{-\chi|v_{rel}|}\right). \end{aligned} \tag{9}$$

The coefficient of friction mentioned in Case 1 describes the classical Coulomb–Amonton friction law which aptly captures the dynamics associated with kinetic friction and is most commonly referenced in literature. However, the coefficient of friction mentioned in Case 2 is more detailed as it not only captures the dynamics associated with kinetic friction, but also captures the dynamics associated with stiction- and Stribeck-effects (which are prominent under dry and lubricated contact conditions respectively).

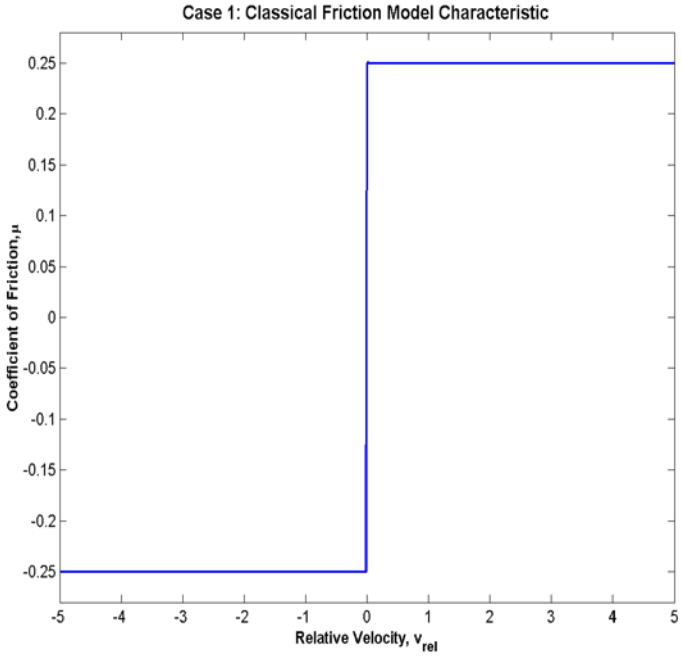

(a)

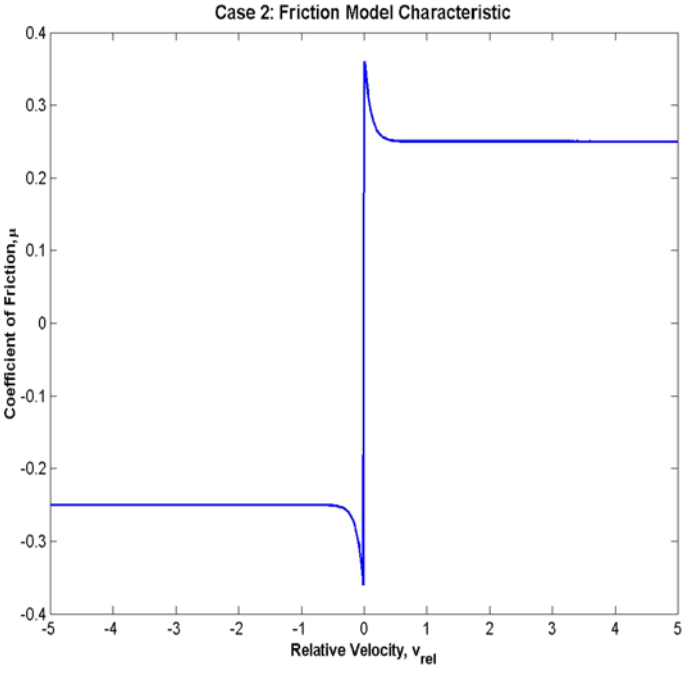

(b)

Fig. 9 Friction characteristics for the contact zone. **a** Case 1: classical friction model, μ vs. v_{rel}. **b** Case 2: analytical friction model, μ vs. v_{rel}

Using continuous (or smooth) friction models and the slip angle, γ (refer to Fig. 5) the normal force (N or λ_N) on the bolt (or pulley) can be obtained as

$$N = F_r \tan\beta + \frac{F_b}{\cos\beta}. \tag{10}$$

Substituting the normal force into (4) and (5) yields a solvable system of equations for the generalized coordinates of the chain CVT system.

3 Results and discussion

A CVT system is continually subjected to torques from both the engine and the final drive inertias. The engine creates an input torque condition on the driver pulley and the final drive exerts a load torque on the driven pulley. The modeling development was done on the MATLAB/Visual C++ platform. The Runge–Kutta method is used to integrate state equations in order to get time histories of the system states. The simulation of a chain-CVT model starts off with an initial condition of rest and a specific design configuration and computes different dynamic performance indices, i.e., axial forces, angular velocities, tension, etc. The driver pulley is subjected to an input torque of 200 Nm whereas a resisting load torque of 100 Nm is applied to the driven pulley. The driver and driven pulleys have constant radii of $r_p = 3$ in. (0.0762 m) and $r'_p = 4.5$ in. (0.1143 m), respectively. However, the links traverse around the pulley grooves in different pitch radii, thereby causing a variation in the transmission ratio. The results corresponding to two different friction characteristics are discussed subsequently. For purposes of brevity, the results will be categorized into two sections:

- Influence of contact-zone friction characteristic (friction + clearance effects)
- Influence of chain link clearance (friction + higher clearance effects)

The chain CVT model is subjected to two different friction characteristics (refer to Fig. 9) that describe the friction between the link and the pulley under different operating or loading conditions. Moreover, clearance-induced nonlinearities, as described by characteristics (A) and (B) in Fig. 8, are also integrated into the CVT model. Table 1 lists the parameter values that define two different clearance models used in the CVT simulation.

3.1 Influence of contact-zone friction characteristic

Figure 10 depicts the time histories of the distance of a chain link from the center of driver pulley for both the cases. The variation in link distance is computed by tracing the position

Table 1 Parameters used for the clearance model

	k_1	p_1	k_2	p_2	k_3	p_3	$\varepsilon_{\min}$	$\varepsilon_{\max}$
Clearance-I	35	1.2	70	2.4	93	3.0	0.00005	0.0001
Clearance-II	0.2	0.015	3	0.3	85	2.5	0.0005	0.001

Units of k: kN/m

Units of p: kN s/m

Units of ε: m

Note: $K_b = 200$ kN/m, $l_b = 0.02$ m

of a link from the center of the driver pulley as the link traverses the different section of the chain CVT, i.e., the free-strands, the driver pulley, and the driven pulley. It can be readily observed from the figure that the chain-link pitch radius on the driver pulley is not the same for all the cases. Figure 11 depicts an exploded view of the variation in the pitch radius of the chain link as it traverses the driver pulley wrap.

As the chain link enters the driver pulley groove, the chain pitch radius decreases. This phenomenon can be attributed to the wedging action between the link and the pulley. However, as the link traverses the pulley wrap, the chain pitch radius increases till the link exits the pulley. This can be attributed to the drop in the tensile force of the link as it moves from the entrance to the exit of the driver pulley. It can be noted from the figure that the chain links travel faster in Case 2 than in Case 1 owing to the presence of a lower resisting load torque (50 Nm) on the driven pulley for Case 2. It was observed (refer to Fig. 12) that a chain CVT under the presence of a friction characteristic governed by Case 2 was unable to sustain a higher load torque of 100 Nm, which was contrary to the load carrying capacity predicted by the classical continuous Coulomb friction law (i.e., under Case 1). Moreover, owing to larger normal force generation in Case 1, the radial path traversed by a chain link in the driver pulley groove is greater in this case than in Case 2. A chain link contacting the driven pulley also shows complementary behavior in the entry and exit phases of its motion.

Figure 13 illustrates the time histories of the normal force between a chain link and the pulley for both the cases. Whenever a chain link comes in contact with the pulley, it exerts a normal force on the sheave, which tends to move the pulley sheaves apart. The pulley normal force has a nonuniform distribution over the contact arc. The normal force increases from the entrance to the exit of the driven pulley, which is in accord with the observations of Ide et al. [30] and Pfeiffer et al. [1, 16]. Moreover, the normal force generated between the driver pulley and the chain link is higher than the normal force generated between the link and the driven pulley. As the chain link wedges into the pulley groove, a significant amount of radial friction force is generated to prevent the inward radial motion of the chain link. Since during the wedging the pitch radius of the chain link decreases on the driver pulley (as depicted in Fig. 11), the link exerts a large normal force on the pulley in order to generate enough torque to compensate for the resisting load on the driven pulley. Since the variations in the pitch radius of the chain on the driven pulley are higher than those over a driver pulley, an adequate amount of normal force between the link and the pulley generates enough friction torque to meet the resisting load torque. It can also be observed from the figure that the normal force generated is lower for Case 2 than for Case 1 because of the lower load torque requirements (50 Nm) on the driven pulley for Case 2 as well as due to the presence of lubrication-related dynamic effects.

Since one of the pulley sheaves is movable, the chain link is capable of exhibiting both tangential and radial motions when it traverses the pulley wrap angle. Consequently, a friction force is generated in the sliding plane, which opposes the relative velocity between the chain link and the pulley. Knowing the sliding direction and the sheave angle, the friction force in the sliding plane can be readily decomposed into radial and tangential components. Figure 14 illustrates the time histories of the tangential friction force for both the cases. The tangential friction force acts as the transmitting force and causes the variations in the tensile force of the chain links. It can be observed from the figure that the tangential friction force between the driver pulley and the link is in anti-phase to the tangential friction phase between the driven pulley and the link. This relationship, in fact, aptly describes the energy transfer interactions between the chain link and the pulleys. It is to be noted that the transmitting force in Case 2 is higher than in Case 1. Since chain links traverse greater radial

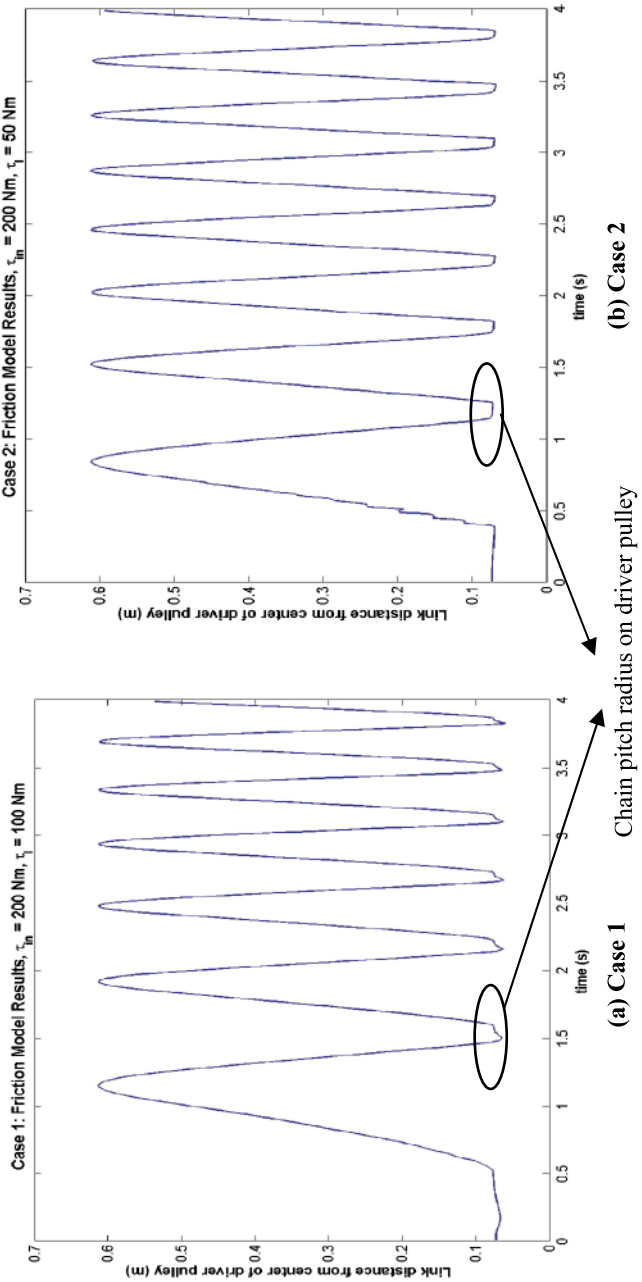

Fig. 10 Time history of link distance from center of driver pulley

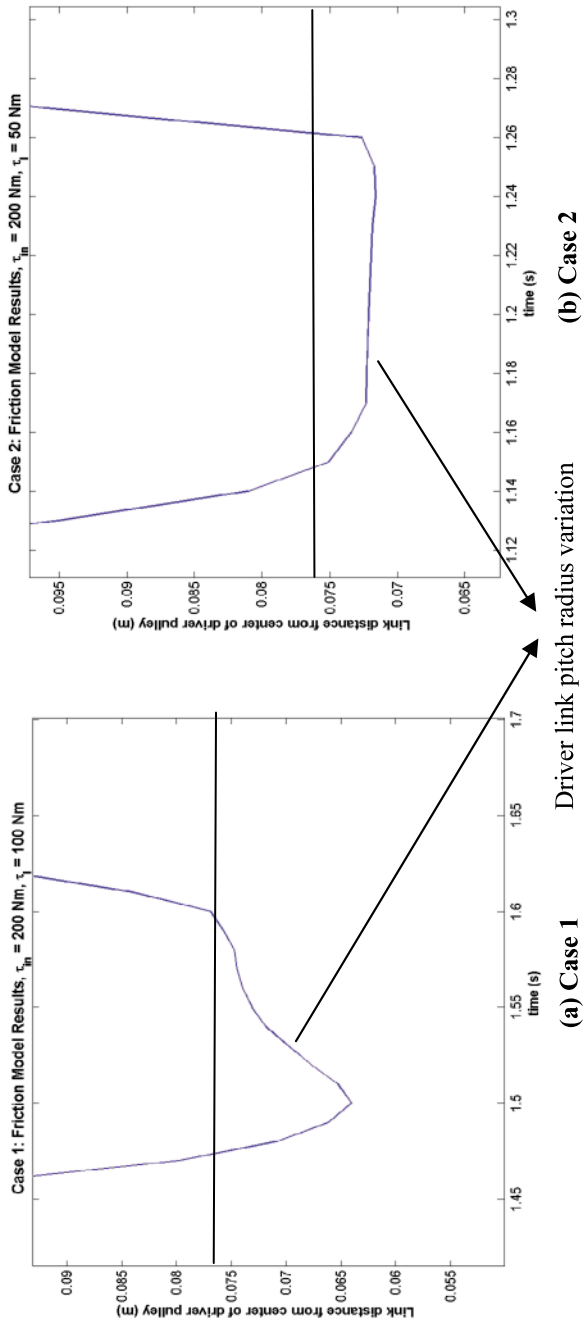

Fig. 11 Exploded view of chain link pitch radius on driver pulley

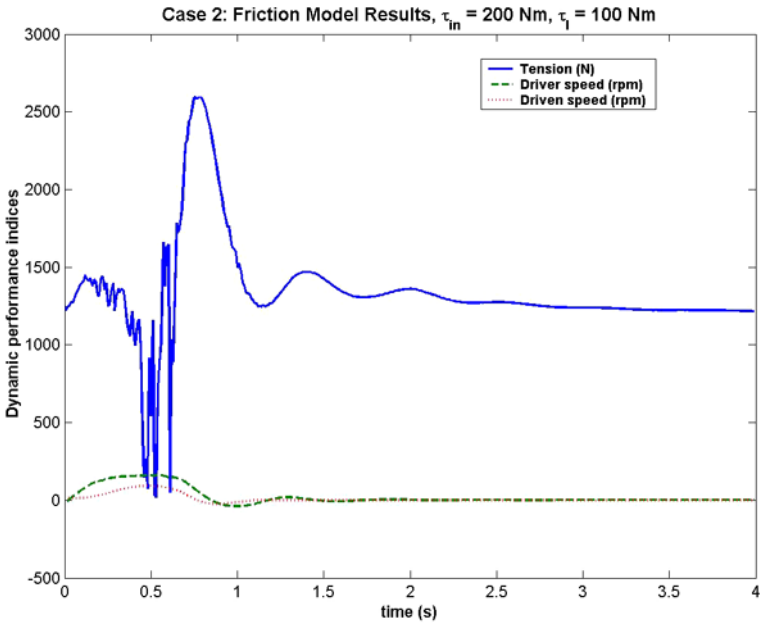

Fig. 12 Time histories of dynamic performance indices (Tension and pulley speeds)—Case 2: Input = 200 Nm, Load = 100 Nm

path in Case 1 than in Case 2, the transmitting force required to overcome the resisting load torque is not high enough for Case 1. It is to be noted from the time histories of normal force and friction force that the chain CVT system exhibit greater wedging losses in Case 2 owing to noisy entrance and exit dynamics over the pulley wraps.

Figure 15 illustrates the time histories of the tensile force in the chain links for both the cases. It is to be noted that the tensile force in the chain links drops as the links traverse the driver pulley wrap from the inlet to the exit of the pulley. On the contrary, the tensile force increases as the links traverse the driven pulley wrap from the inlet to the exit of the pulley. Moreover, with passage of time, the tensile force in the chain links increases. It can also be noted from the figure that the link tension exhibits significant variations as the link passes through the entry and exit regions of the pulleys for a CVT system with friction described by Case 2. This not only degrades the system performance, but also induces irregular behavior in the system, which might be difficult to control. Moreover, since the transmitting force required to meet the load torque is higher for Case 2, the tensile force in the chain links with friction described by Case 2 is higher is in comparison to the tensile force generated in Case 1. It is plausible from the plots that a CVT system with the classical continuous Coulomb friction characteristic (i.e., Case 1) is able to transmit torque much more smoothly than a CVT system with friction characteristic governed by Case 2.

As mentioned previously, the pulleys are subjected to torque-loading conditions. An input torque is applied to the driver pulley, whereas the driven pulley is subjected to an opposing load torque. The links and the pulleys start off from a zero initial velocity configuration, and the angular speeds of the pulleys are recorded during the simulation. Figure 16 illustrates the time histories of the pulley angular speeds. It can be inferred from the plots that the CVT system entails greater losses in Case 2 than in Case 1, as in spite of a low load torque of 50 Nm, it is not able to generate enough friction torque to rev up the driven pulley.

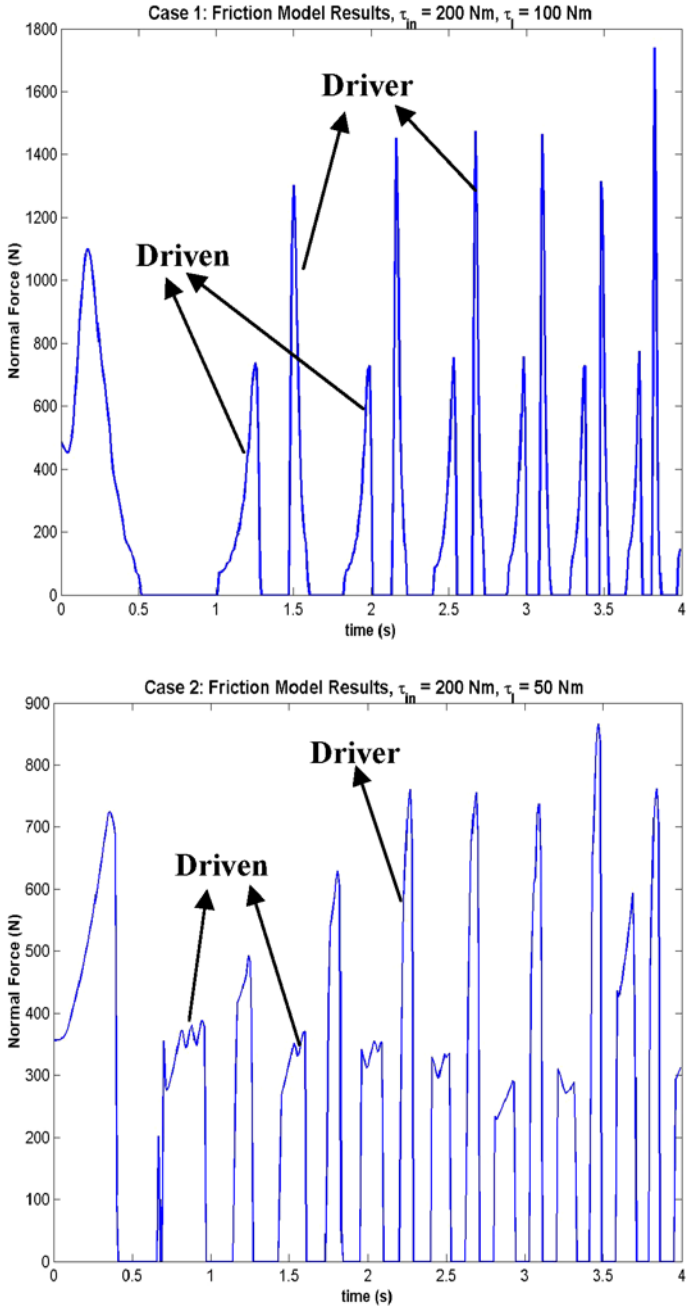

Fig. 13 Time history of pulley normal force

However, there is a greater difference between the driver and driven pulley speeds for Case 1 than for Case 2. This can be attributed to the greater radial penetration of chain links in the pulley groove under the friction characteristic described by Case 1. Consequently, the

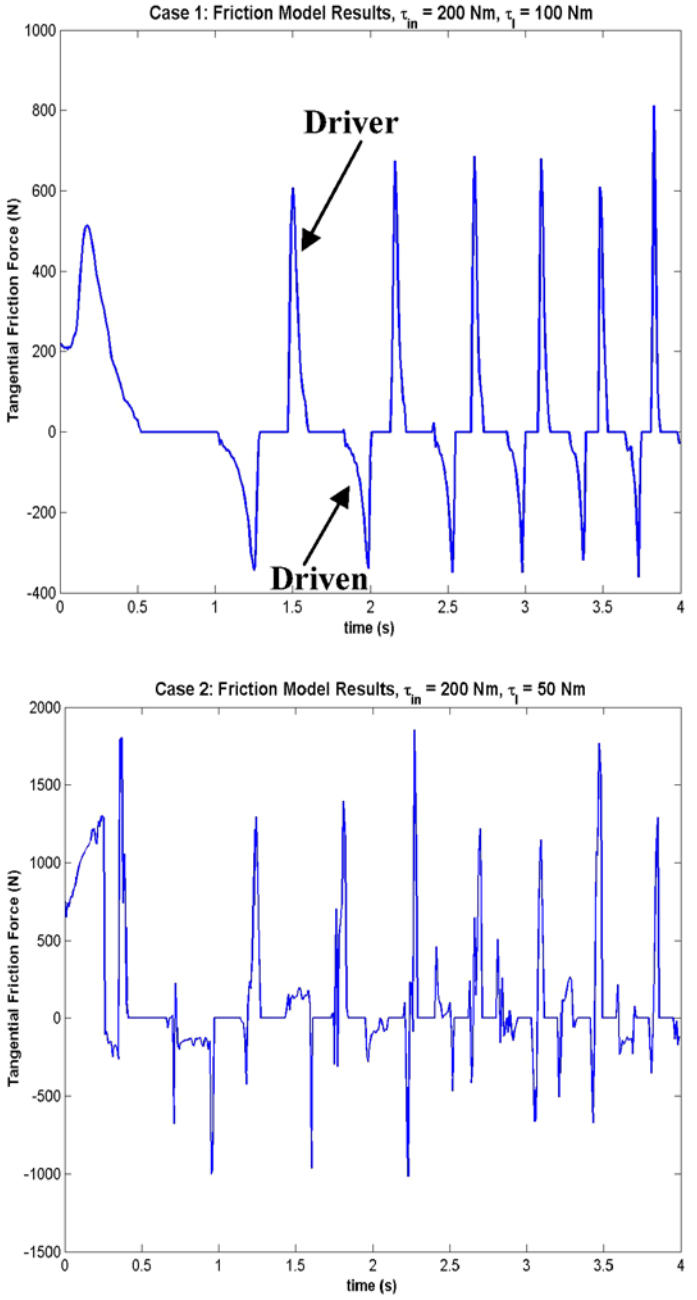

Fig. 14 Time history of tangential friction force

friction torque on the driver pulley decreases (thereby, increases in driver pulley speed), whereas it increasingly resists the load torque on the driven pulley (due to increasing chain pitch radius on the driven pulley).

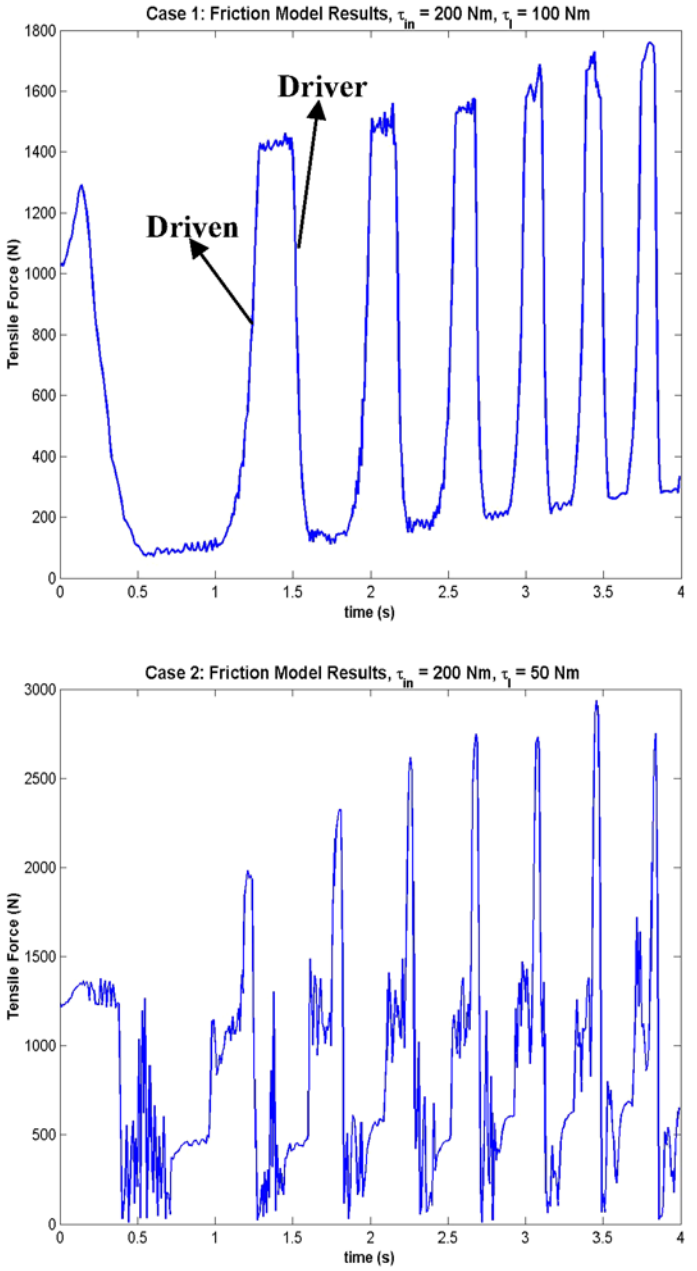

Fig. 15 Time history of link tensile force

As the chain link moves around the pulleys, it exerts a force in the axial direction on the pulley sheave. The link moves radially inwards and outwards within the pulley groove, which causes variations in the transmission ratio. The axial force generated along the pulley shaft is computed from the bolt force, as discussed in the previous section. Figure 17

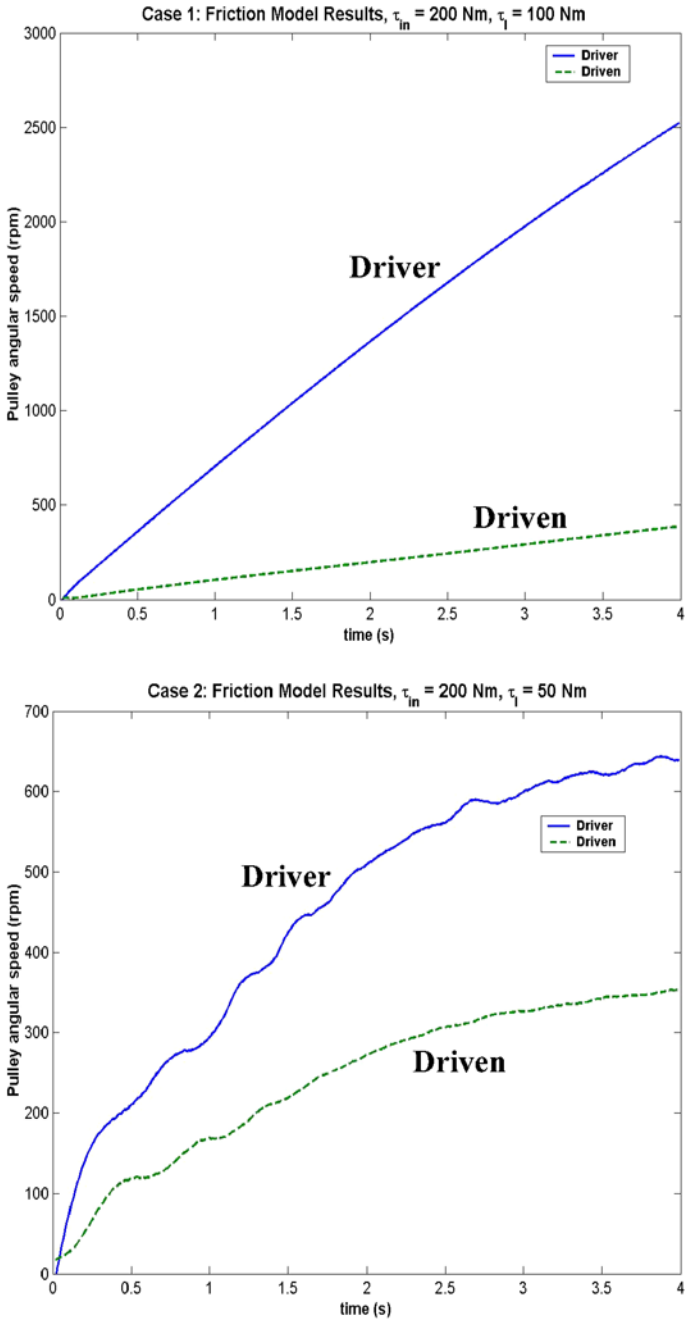

Fig. 16 Time history of pulley angular speeds

illustrates the time histories of the axial forces on the driver pulley for both the cases. Similar trends can be observed for the axial force on the driven pulley sheave. It can be

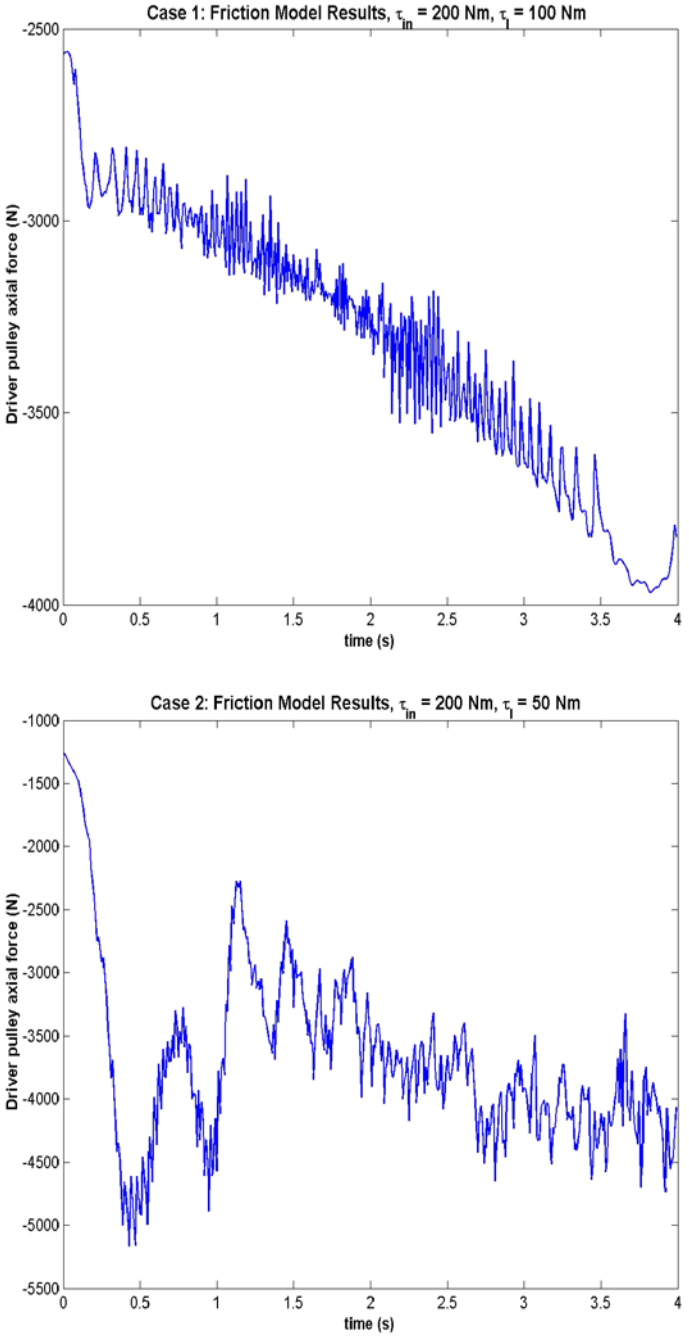

Fig. 17 Time history of driver pulley axial force

noted from the figure that the system is unable to generate more axial force after some time for Case 2. The pulley sheaves, in fact, begin to experience medium-amplitude oscillations which degrade the dynamic performance and lower the torque transmitting capacity of the system.

3.2 Influence of chain link clearance

The response of a CVT changes considerably under the influence of clearance between the chain links, which may be inherent or may arise during its continual operation. As discussed previously, clearance-induced nonlinearities are taken into account through the piecewise stiffness elements between the chain links. The two significant parameters in the clearance model that drastically influence the system dynamics are (k, p) and ε. The results presented in the previous section were obtained under the influence of different friction characteristics and clearance-I (refer to Table 1) model parameters. In order to understand the impact of clearance on system dynamics, clearance-II model parameters are now introduced in the chain CVT model. As can be noted from Table 1, clearance-II model parameters manifest system dynamics under high clearance (which plausibly reflects a situation of large wear in the system). Figure 18 illustrates the time histories of link tensile force, driven pulley speed, and driver pulley axial force for a CVT system under the contact-zone friction characteristic of Case 1 (refer to (9)) and the loading conditions of 200 Nm input torque and 100 Nm load torque on the driver and driven pulleys, respectively. It can be noted from the time history of the tensile force of the chain links that the links undergo significant high-frequency vibrations in the free strands and the entry and exit regions of the pulleys in the chain CVT system. Owing to significant wedging losses, a part of the friction torque needed to overcome the load torque on the driven pulley is also lost or dissipated. Consequently, the driven pulley speed is seen to be lower in comparison to the earlier case (refer to Fig. 16). Although the links were able to generate sufficient forces to meet the load torque, the pulley sheaves could undergo chattering due to high-frequency chaotic or quasi-periodic oscillations, which are perilous to the CVT system. It was observed that as the slope parameters of the clearance-model were increased, such high-frequency chattering phenomena were circumvented, the transmission efficiency increased, and torque transmissibility also enhanced. Thus, owing to higher clearance effects, the same CVT system under the influence of continuous Coulomb friction characteristic has torque-carrying capacity lower than it had earlier. Thus, it is the combined nonlinear effect of friction and clearance that influences the torque-transmitting capacity of a chain CVT system.

4 Conclusions

The paper outlined a detailed planar multibody model of a chain CVT under the influence of clearance between the chain links and two different friction characteristics (that describe the friction between the chain link and the pulley). Since excitation mechanisms exist due to the impact and polygonal action of chain links in a chain CVT, it is necessary to model the chain CVT as a multibody system in order to accurately capture the dynamics arising from its discrete nature. A chain CVT falls under the category of friction-limited drives and depending on different operating (or loading) conditions and design configurations, the friction characteristic of the contacting components of a CVT may vary. For instance, in the case of a fully lubricated CVT, the friction characteristic of the contacting surface may bear a resemblance to the Stribeck curve rather than to a continuous Coulomb characteristic.

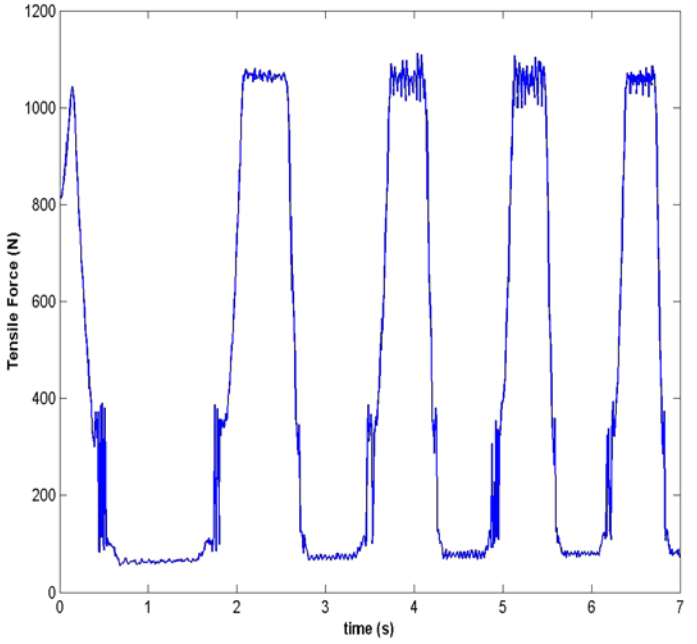

(a)

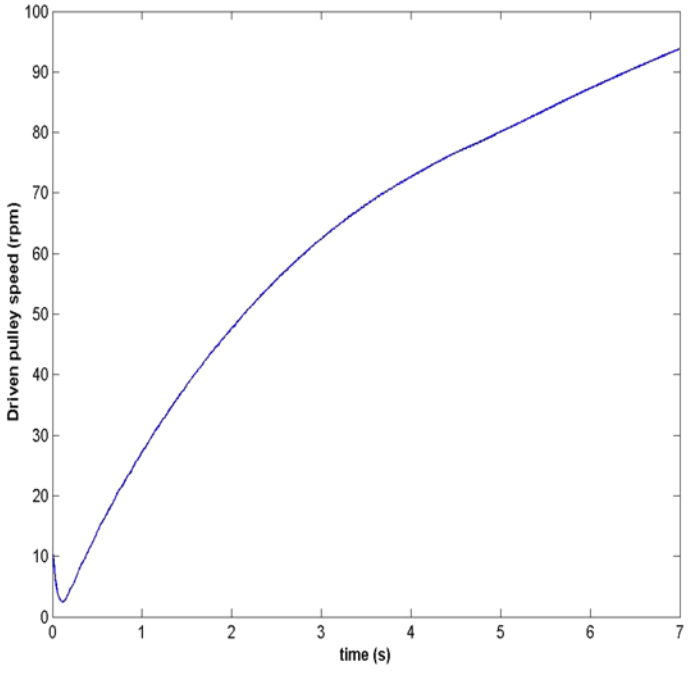

(b)

Fig. 18 Dynamic performance indices under high clearance—Case 1. **a** Tensile force vs. time—Case 1. **b** Driven pulley speed vs. time—Case 1. **c** Driver pulley axial force vs. time—Case 1

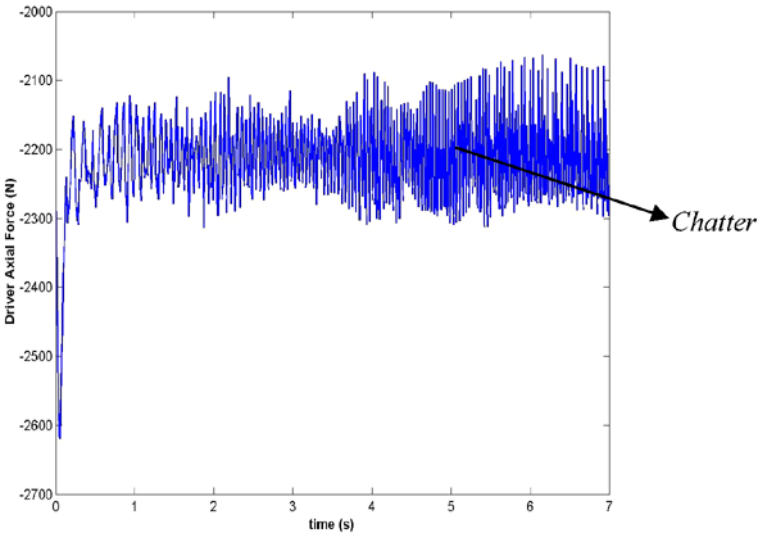

(c)

Fig. 18 continued

With the aim of understanding friction-related dynamics, two realistic physics-based mathematical models of friction were incorporated to describe friction between the link and the pulley. The friction characteristic in Case 2 is able to capture not only the kinetic friction effects (as in Case 1), but also effects similar to stiction and boundary-lubrication. It was observed that the torque carrying capacity of the CVT system lowered under the presence of friction characteristic as described by Case 2. Moreover, the chain CVT entails greater losses from noise, vibration, and wedging of the chain links in Case 2 than in Case 1. The variation in the transmission ratio is also higher for Case 1 than for Case 2. It is evident from the results that, as a highly nonlinear system, CVT is capable of exhibiting varied performance under different friction characteristics of the contact zone between the link and the pulley. It is also plausible for the system to undergo chaoticity which not only hampers the torque transmission but also makes it difficult to be controlled. So, the performance of a CVT can vary drastically from the condition of dry friction to a fully-lubricated condition.

As mechanical systems wear, clearances between mating surfaces develop that can fundamentally change the behavior of the system and also induce unnecessary noise and vibrations. A CVT is no exception, and over continual operation it is susceptible to form clearances between its components. Moreover, it is quite possible for a CVT to have clearances among its various components during the assembly process. These clearances influence the dynamic behavior, torque capacity, and life of a CVT. Clearance inherently is a non-smooth nonlinearity (may be piecewise linear), which makes the CVT system non-smooth too. A piecewise force-element model is embedded into the multibody model of chain CVT in order to capture the effects of clearance on system performance. It was observed that clearance parameters drastically influence the performance of the CVT system, sometimes even rendering the operation perilous. The higher the clearance between the chain links, the lower is the torque transmissibility and the higher are the transmission losses. It was also observed that lower slope parameter in the clearance model (i.e., lower stiffness and damping factors of the interconnecting force elements) may render the system unstable. So, even

though the clearance between the links is low, a low stiffness in the interconnecting force element can create instability in the CVT system. Clearance also induces high-frequency quasi-periodic or chaotic vibrations, which are difficult to control and can cause early wear of the system. Since clearance has two effects, i.e., elongation of the chain links and the contact/detachment transitions between the links, further parameter-based investigation is necessary to understand the dynamics of a clearance-dominated chain CVT system under several operating or loading conditions.

A more accurate analysis of the torque transmissibility of a chain CVT system can be done by modeling the links as elastic bodies, accounting for spatial orientation of the chain links (using a spatial model), and by developing a finite element model for elastic deformations in the pulley sheave. However, since the primary goal of this research was to study the influence of clearance and friction-related nonlinearities on the dynamic performance of a chain CVT, a planar chain CVT with an approximate pulley-bending model suffices. It is also important to note that although exact knowledge of the friction characteristic in a CVT system can only be obtained by real-time monitoring of the contact patch dynamics in a production CVT, these mathematical models give profound insight into the probable behavior that a CVT system exhibits under different operating conditions, which may be further exploited to design efficient CVT controllers to analyze the noise and vibration behavior of a CVT-loaded powertrain or vehicle, etc. It is also to be noted that the friction model presented in this research is a static-based friction model as the stiction is represented approximately by the conditions of negligible relative velocity. A more accurate analysis of the contact conditions can be done either by using a friction model that accounts for not only the effects of relative velocity, but also the effects of relative acceleration between two contacting surfaces, or by using linear complementarity formulations. The research reported in this paper shows that not only the dynamic performance and torque capacity of a CVT can decrease in the presence of nonlinearities such as friction and clearance, but also the system can exhibit irregular or chaotic behavior that may prove to be perilous to the system over time. However, further investigation by exploiting the tools from nonlinear dynamics and chaos like Lyapunov exponents, Poincaré maps, etc., is necessary to corroborate the transmission trends reported in this paper.

Acknowledgements This research was supported by the Automotive Research Center (ARC), a US Army TACOM Center of Excellence for Modeling and Simulation of Ground Vehicles. The support and interest of our sponsors is gratefully acknowledged.

References

1. Srnik, J., Pfeiffer, F.: Dynamics of CVT chain drives. Int. J. Veh. Des. **22**(1/2), 54–72 (1999)
2. Ravn, P.: A continuous analysis method for planar multibody systems with joint clearance. Multibody Syst. Dyn. **2**, 1–24 (1998)
3. Pedersen, S.L., Hansen, J.M., Ambrósio, J.A.C.: A Roller chain drive model including contact with guide-bars. Multibody Syst. Dyn. **12**, 285–301 (2004)
4. Flores, P., Ambrósio, J., Claro, J.P.: Dynamic analysis for planar multibody mechanical systems with lubricated joints. Multibody Syst. Dyn. **12**, 47–74 (2004)
5. Kobayashi, D., Mabuchi, Y., Katoh, Y.: A study on the torque capacity of a metal pushing V-belt for CVTs. In: SAE Transmission and Driveline Systems Symposium. SAE Paper No. 980822 (1998)
6. Micklem, J.D., Longmore, D.K., Burrows, C.R.: Modelling of the steel pushing V-belt continuously variable transmission. Proc. Inst. Mech. Eng. Part C **208**, 13–27 (1994)
7. Sun, D.C.: Performance analysis of a variable speed-ratio metal V-belt drive. Trans. ASME Mech. Transm. Automot. Des. **110**, 472–481 (1988)
8. Carbone, G., Mangialardi, L., Mantriota, G.: Influence of clearance between plates in metal pushing V-belt dynamics. Trans. ASME J. Mech. Des. **124**, 543–557 (2002)

9. Srivastava, N., Haque, I.: On the transient dynamics of a metal pushing V-belt CVT at high speeds. Int. J. Veh. Des. **37**(1), 46–66 (2005)
10. Srivastava, N., Haque, I.U.: On the operating regime of a metal pushing V-belt CVT under steady state microslip conditions. In: 2004 International Continuously Variable and Hybrid Transmission Congress, San Francisco, USA, 23–25 September 2004. Paper No. 2004-34-2851 (04CVT-11) (2004)
11. Srivastava, N., Blouin, V.Y., Haque, I.U.: Using genetic algorithms to identify initial operating conditions for a transient CVT model. In: 2004 ASME International Mechanical Engineering Congress, Anaheim, CA, USA, 13–19 November 2004. Paper No. IMECE2004-61999 (2004)
12. Srivastava, N., Haque, I.: Transient dynamics of metal V-belt CVT: effects of pulley flexibility and friction characteristic. ASME J. Comput. Nonlinear Dyn. **2**(1), 86–97 (2007), Paper No. CND-06-1084
13. Srivastava, N., Haque, I.: Influence of clearance on the dynamics of chain CVT drives. In: 2006 ASME International Mechanical Engineering Congress, Chicago, IL, USA, 5–10 November 2006. Paper No. IMECE2006-14059 (2006)
14. Srivastava, N., Haque, I.: Influence of friction characteristic on the performance of chain CVT drives. J. KONES Powertrain Transp. **13**(2), 405–419 (2006)
15. Fawcett, J.N.: Chain and belt drives—a review. Shock Vib. Dig. **13**(5), 5–12 (1981)
16. Srnik, J., Pfeiffer, F.: Simulation of a CVT chain drive as a multibody system with variant structure. In: Proceedings of the 1st Joint Conference of International Simulation Societies, Zurich, Switzerland, 22–25 August 1995, pp. 241–245 (1995)
17. Fritz, P., Pfeiffer, F.: Dynamics of high speed roller chain drives. In: 1995 ASME Design Engineering Technical Conferences, DE-Vol. 84-1, vol. 3, Part A, Boston, MA, USA, 17–21 September 1995, pp. 573–584 (1995)
18. Sedlmayr, M., Bullinger, M., Pfeiffer, F.: Spatial dynamics of cvt chain drives. In: Proceedings of CVT 2002 Congress, VDI-Berichte, 1709, Düsseldorf, Germany, pp. 511–552 (2002)
19. Pfeiffer, F., Sedlmayr, M.: Force reduction in CVT chains. Int. J. Veh. Des. **32**(3/4), 290–303 (2003)
20. Sattler, H.: Efficiency of metal chain and V-belt CVT. In: Int. Congress on Continuously Variable Power Transmission CVT' 99, Eindhoven, The Netherlands, 16–17 September 1999, pp. 99–104 (1999)
21. Pfeiffer, F., Lebrecht, W., Geier, T.: State-of-the-art of CVT-modelling. In: 2004 International Continuously Variable and Hybrid Transmission Congress, San Francisco, USA, 23–25 September 2004. Paper No. 04CVT-46 (2004)
22. Tenberge, P.: Efficiency of chain-CVTs at constant and variable ratio: a new mathematical model for a very fast calculation of chain forces, clamping forces, clamping ratio, slip, and efficiency. In: 2004 International Continuously Variable and Hybrid Transmission Congress, San Francisco, USA, 23–25 September 2004. Paper No. 04CVT-35 (2004)
23. Lebrecht, W., Pfeiffer, F., Ulbrich, H.: Analysis of self-induced vibrations in a pushing V-belt CVT. In: 2004 International Continuously Variable and Hybrid Transmission Congress, San Francisco, USA, 23–25 September 2004. Paper No. 04CVT-32 (2004)
24. Carbone, G., Mangialardi, L., Mantriota, G.: EHL visco-plastic friction model in CVT shifting behaviour. Int. J. Veh. Des. **32**(3/4), 333–357 (2003)
25. Canudas de Wit, C., Olsson, H., Åström, K.J., Lischinsky, P.: Dynamic friction models and control design. In: Proceedings of the 1993 American Control Conference, San Francisco, CA, USA, pp. 1920–1926 (1993)
26. Pfeiffer, F., Glocker, C.: Multibody Dynamics with Unilateral Contacts. Wiley–Interscience, New York (1996)
27. Sorge, F.: Influence of pulley bending on metal V-belt mechanics. In: Proceedings of International Conference on Continuously Variable Power Transmission, Japanese Society of Automotive Engineers, Yokohama, Japan, 11–12 September 1996. Paper No. 102 (9636268), pp. 9–15 (1996)
28. Carbone, G., Mangialardi, L., Mantriota, G.: The influence of pulley deformations on the shifting mechanism of metal Belt CVT. In: Trans. ASME J. Mech. Des. **127**, 103–113 (2005)
29. Sferra, D., Pennestri, E., Valentini, P.P., Baldascini, F.: Dynamic simulation of a metal-belt CVT under transient conditions. In: Proceedings of the DETC02, 2002 ASME Design Engineering Technical Conference, Montreal, Canada, 29 September–2 October 2002. Paper No. DETC02/MECH-34228, vol. 5A, pp. 261–268 (2002)
30. Ide, T., Tanaka, H.: Contact force distribution between pulley sheave and metal pushing V-belt. In: Proceedings of CVT 2002 Congress. VDI-Berichte, vol. 1709, pp. 343–350 (2002)